STRENGTH OF SOUTHERN PINE 2 x 4 BEAM-COLUMNS

By

JOHN J. ZAHN

May 1984

STUDY COMPLETION REPORT
FOR RELEASE THROUGH NTIS

STRENGTH OF SOUTHERN PINE 2 x 4 BEAM-COLUMNS

John J. Zahn

United States Department of Agriculture

Forest Service

Forest Products Laboratory

Post Office Box 5130
Madison, WI 53705

May 1984

ABSTRACT

This paper presents a finite element program, Ultimate Strength of Beam-Columns (USBC), able to simulate the destructive testing of in-grade lumber under combined bending and compression. It also presents two kinds of test data on southern pine 2 x 4's: tests of short members provide an input properties distribution for USBC, and tests of full-length members in seven groups of various lengths and grades provide verification data to evaluate the performance of USBC. The simulator USBC reproduced the mean and variance of each group very well, especially for shorter, lower grade members. It is somewhat conservative for longer, higher grade members but this is deemed acceptable because these cases can be designed as homogeneous elastic bodies. The simulator was then employed to study the interaction of bending and compression in each of the seven groups of full-length members by simulating the testing of each piece under many combinations of moment and axial load. The results demonstrate the conservatism of the linear interaction equation used in timber design, especially at shorter lengths and lower grades. This is important to the efficient design of wood beam-columns such as wall studs and truss chords.

Key Words: Wood, timber, beam-columns, southern pine, interaction equation.

CONTENTS

STRENGTH OF SOUTHERN PINE 2 x 4 BEAM-COLUMNS

By

JOHN J. ZAHN, Research General Engineer
Forest Products Laboratory[1]

INTRODUCTION

New design criteria for roof trusses and stud walls will be based on whole-system analyses of roofs and walls. Such analyses need an accurate failure criterion for wood members subjected to combined bending and compression. This study and an earlier study of western hemlock 2 x 6's (Zahn 1982) are aimed at meeting that need.

The main difficulty in studying the strength of lumber under combined load is that each member can be tested to destruction only once. Hence to measure strength at several different load combinations one must replicate each test many times and examine mean values. If, in addition, one wishes to study the effects of other variables such as member length, lumber grade, cross section size, and species, a purely experimental approach becomes very costly and time consuming. Therefore a computer simulator was developed in Zahn 1982 that can simulate the strength of a given member under any combination of bending and compression. By repeated simulation of the same member under different load combinations a complete interaction curve can be generated for each member. If this is done for a representative random sample, the mean value of the simulated interaction curves can be taken as representative of that length, grade, size, and species. In this study, size and species were fixed and length and grade were varied.

---

[1]The Laboratory is maintained in cooperation with the University of Wisconsin.

I had three objectives in this study:

1. to examine the strength of southern pine 2 x 4 lumber
2. to develop and verify an improved finite-element simulator, and
3. to study the interaction of bending and compressive strength at several lengths and grades.

The new computer simulator is called USBC for Ultimate Strength of Beam-Columns. USBC is a nonlinear, finite-element program whose input is a distribution of single-element properties capable of specifying the complete nonlinear moment-curvature relationship of each element as a function of specified quality indices and load ratio (ratio of moment M to axial compression P). The quality indices chosen for this study were edgewise modulus of elasticity (EMOE) and visual quality rating (VQR). The previous study (Zahn 1982) of western hemlock used only one quality index, E_r, an edgewise modulus of elasticity that included the effects of shear deformations in the two adjoining elements.

In addition to obtaining single-element data for input to USBC, data were obtained on seven groups of full length lumber to verify the ability of USBC to accurately reproduce the effects of length and grade. The previous study had only one group of 8-foot members as a verification and it was found that mean strength could be accurately modeled but that variability was seriously underestimated.

FINITE ELEMENT SIMULATION

Because a finite-element program can simulate a complete interaction curve of strength under combined bending and compression, it will yield more reliable information about the shape of the interaction curve than a purely experimental study would, provided that the accuracy of the simulator has been adequately verified. Each member to be simulated is first marked off into 12-inch "elements" and each element is rated for quality. During simulation the element size must remain fixed. To make the program as accurate as possible, a nonstandard finite-element method was employed in which the nonlinear moment-curvature relationship is exactly satisfied within each element and deflections and slopes are matched at the nodes between elements. The method has been described in detail (Zahn 1982) and will only be sketched here.

Method

Because failure under combined loading is essentially a bending failure, the element behavior is modeled as one of bending conditioned by the simultaneous presence of axial compression. That is, the basic material properties are those that describe the moment-curvature relationship of an element, but these properties are made functionally dependent upon the load ratio M/P (nominal bending moment over compressive force). Because all of the combined load tests in this study are eccentric axial load tests, the load ratio is always equal to the eccentricity of the axial load. That is, in axial load tests

$$M = Pe \tag{1}$$

where M = nominal moment, P = axial force, and e = eccentricity.

The actual moment-curvature relationship is represented by a Ramberg-Osgood function (Ramberg and Osgood 1943):

$$\frac{c}{R} = \frac{Mc}{EI} + K\left(\frac{Mc}{EI}\right)^n \tag{2}$$

where c = half depth = 1.75 inches, EI = flexural rigidity lb/in.^{2}, and K and n are fitted parameters. To minimize rounding error in the curve fitting computations equation 2 was written in the form

$$\frac{c}{R} = \chi + \exp\left[\ell n\ (y_u) + n\ \ell n\ \left(\frac{\chi}{\chi_u}\right)\right] \tag{3}$$

where $\chi \equiv \frac{Mc}{EI}$, $\chi_u = \chi$ at ultimate load, and $y_u \equiv \frac{c}{R} - \frac{Mc}{EI}$ at ultimate load. This form explicitly displays four properties as fitted parameters: EI = stiffness, χ_u = strength, y_u = ductility, and n = knee shape. These four parameters provide a four-dimensional material property vector $\underline{F}$ that completely specifies the curve of actual moment versus curvature of the element.

$$\underline{F} \equiv \begin{bmatrix} EI \\ \chi_u \\ y_u \\ n \end{bmatrix} \tag{4}$$

These single-element data were fitted with a multivariate normal distribution. I tried several data transformations and found that $\underline{Y}$ is more nearly normal than $\underline{F}$ where

$$\underline{Y} \equiv \begin{bmatrix} \ell n(EI \times 10^{-6}) \\ \ell n\ M_u \\ \ell n\ y_u \\ \ell n\ \ell n\ n \end{bmatrix} \tag{5}$$

This has the further advantage of ensuring that $\underline{F}$ is positive, as it must be by definition. Thus, given the 4-vector $\underline{Y}$ for each element, the simulator constructs the complete moment-curvature relationship of each element. The solution method employs a linear secant relationship which is iterated until the exact nonlinear relationship is satisfied. The load is initially small and is increased by small increments until one element fails.

As the load increases, the deflection of each element increases, thereby changing the eccentricity of the element. But because $\underline{Y}$ is a function of eccentricity, the simulator iterates until that functional relationship is also exactly satisfied. Figure 1 shows a block diagram of the computing method.

Specification of Element Properties

Element properties are not directly specified at input. Rather, element quality $\underline{X}$ is specified at input and element properties $\underline{Y}$ are inferred from $\underline{X}$. Element quality is defined by the nondestructive measures:

$$\underline{E} = \begin{bmatrix} VQR \\ \\ EMOE \end{bmatrix} \tag{6}$$

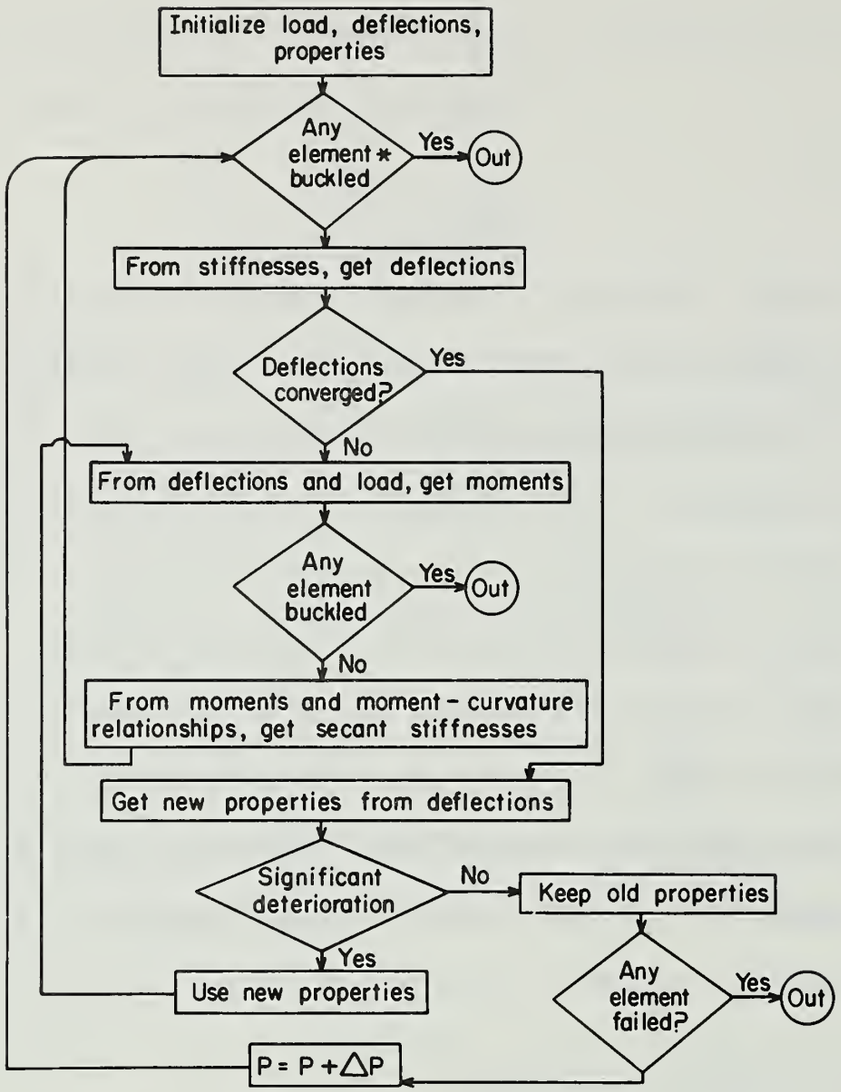

Figure 1.--Block diagram of simulation program USBC. The program also checks at * for numeric instability (endless oscillations) (ML845424).

where EMOE = edgewise modulus of elasticity of an element and VQR = visual quality rating. This vector $\underline{E}$ was transformed to $\underline{X}$ where

$$\underline{X} \equiv \begin{bmatrix} \text{VQR} - 7 \\ \ell n(\text{EMOE} \times 10^{-6}) - 0.45 \end{bmatrix} \qquad (7)$$

because $\underline{Y}$ correlates better with $\underline{X}$ than with $\underline{E}$. Here the values 7 and 0.45 were chosen to make the mean of $\underline{X}$ approximately zero. This has advantages that will be discussed further in Experimental Results--Single-Element Data.

Given $\underline{X}$ the simulator infers $\underline{Y}$, either deterministically or probabilistically. If probabilistically, $\underline{Y}$ is randomly selected from a distribution dependent upon $\underline{X}$ and the simulation is repeated many times for each member until an output distribution of failing loads is obtained (Monte Carlo simulation). If deterministically, $\underline{Y}$ is a single valued function of $\underline{X}$ and each member is simulated only once. Three schemes were investigated in this study and in Zahn 1982:

1. Input a joint distribution for $\underline{Y}$ and $\underline{X}$. Then given $\underline{X}$, form a conditional distribution of $\underline{Y}$. This scheme and Monte Carlo simulation were used in Zahn 1982.
2. Input a linear regression of the mean of $\underline{Y}$ onto $\underline{X}$:

$$\overline{\underline{Y}} = \underline{\underline{A}}\ \underline{X} + \underline{B} \tag{8}$$

   and also input a covariance matrix of $\underline{Y}$ assumed to be independent of $\underline{X}$. This scheme with Monte Carlo simulation was originally tried in this study and rejected.
3. Input a deterministic relationship

$$\underline{Y} = \underline{\underline{A}}'\ \underline{X} + \underline{B}' \tag{9}$$

   and simulate each member only once. This is the scheme finally adopted in this study, with $\underline{\underline{A}}'$ and $\underline{B}'$ fitted by orthogonal least squares.

In each of these schemes the functional dependence of $\underline{Y}$ upon eccentricity e can be handled by making each statistic S_i in the relationship of $\underline{Y}$ to $\underline{X}$ a function of e:

$$S_i = f_i (e), \; i = 1, \; m \tag{10}$$

where f_i = a suitably chosen function fitted to data obtained at several eccentricities and m = the number of statistics needed to specify $\underline{Y}$ ($\underline{X}$). The dependence of $\underline{Y}$ upon $\underline{X}$ and e is discussed further under Experimental Results--Single-Element Data.

EXPERIMENTAL PROCEDURES

Material Selection

Kiln dried southern pine 2 x 4's were purchased in two lots. The first lot, for single-element tests, was selected with the aid of a portable dynamic E rating machine to have the widest possible range of quality. Boards 10 or 12 feet long were chosen so that at least one 54-inch-long test specimen could be cut from each board with a grade-reducing defect in the center 12-inch gage length. The second lot consisted of representative samples of 40 boards each in seven groups (table 1).

Single-Element Tests (short members)

Twelve inches was deemed to be the smallest feasible gage length for measuring curvature in a 2 x 4. To establish the distribution of element properties, a gage length of 12 inches in the center of a 4.5 foot test member was subjected to eccentric axial load (fig. 2). Specimens were divided into

Table 1.--Design of verification experiments

Member length	Gage length	Grade			Group[1]
		1	2	3	
- - - Ft - - - -		Number of specimens			
8	5		40	40	5, 6
10	7	40		40	7, 8
12	9		40		9
14	11	40	40		10, 11

[1]Groups 1 to 4 are in table 2.

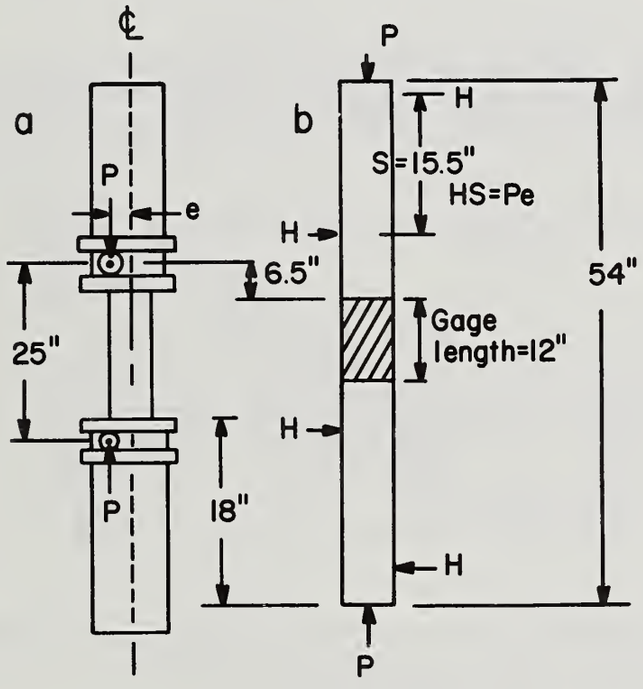

Figure 2.--Diagram of (a) eccentric axial load applied to boots (hollow grips) with test member inside, and (b) test member showing contact forces exerted by boots. Distance S (15.5 in.) was large enough to prevent H from causing shear failure in boot (ML845426).

four groups and tested at different eccentricities (table 2). One group (pure bending) was tested under two point loading (fig. 3).

Table 2.--Design of experiments on 54 inch 2 x 4's to establish element property distribution

Group	1	2	3	4
	- - - - - - - In. - - - - - - - -			
Eccentricity	0.65	1.00	2.25	∞[1]
Sample size	135	135	135	135
Net sample size[2]	112	128	121	118

[1]Group 4 tested in pure bending.
[2]After discarding members that failed in the grips or outside gage length.

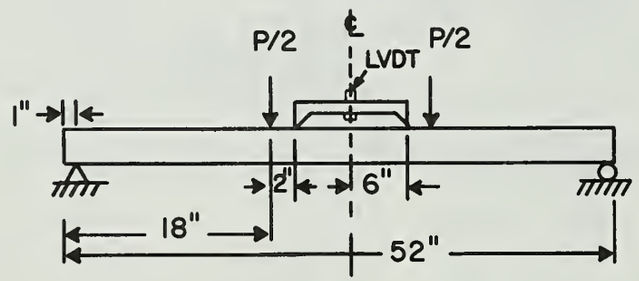

Figure 3.--Pure bending test with specimens of group 4. Same test set-up was used to nondestructively measure edgewise modulus of elasticity (EMOE) of all specimens in groups 1 to 4 (ML845427).

Quality rating.--Before testing to destruction, each 12 inch gage length was rated for quality in two ways.

1. The edgewise modulus of elasticity (EMOE) was measured in a non-destructive bending test (fig. 3). The total load was limited to 135 lb, and

curvature was measured by setting a 12-inch bridge on top of the specimen with a linear variable differential transformer (LVDT) at center span (fig. 4). The curvature is inferred from the LVDT reading by

$$\frac{1}{R} = \frac{2y}{a^2} \tag{11}$$

where R = radius of curvature, y = LVDT reading, and 2a = bridge span (12 in.).

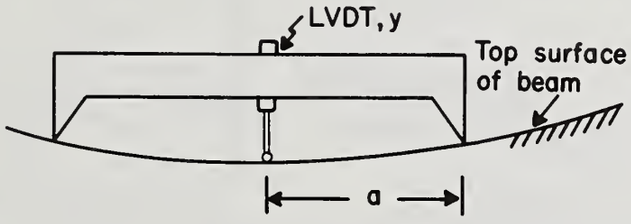

Figure 4.--Bridge used to measure curvature. Bridge rested on top surface of test member and detected changes in curvature from changes in linear variable differential transformer (LVDT) readings (ML845428).

2. A visual quality rating (VQR) was assigned using a scale of 1 to 10 developed by C. Gerhards (1983).

These indices provide a two-dimensional quality vector $\underline{E}$ in equation 6 above. So that all four groups would have nearly identical distributions of quality $\underline{E}$, the specimens were first sorted in order of increasing value of Q where

$$Q \equiv VQR + EMOE \times 10^{-7} \tag{12}$$

This sorted the members into groups by integer value of VQR. Within each group EMOE increased monotonically. The first four specimens with smallest values of Q were then randomly assigned to groups 1 to 4. Then, the next four

were randomly assigned, and the next four, etc., until four matched groups were produced. Resulting histograms of all four groups were nearly identical. The common histograms of VQR and EMOE are shown in figure 5.

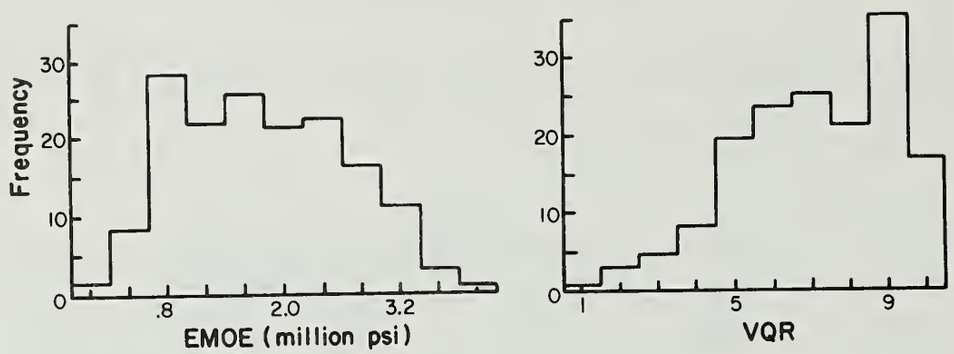

Figure 5.--Histograms of visual quality rating (VQR) and edgewise modulus of elasticity (EMOE) for groups 1 to 4 (ML845429).

Strength tests.--Grips used for western hemlock 2 x 6's (Zahn 1982) were modified for use with 2 x 4's. The loose bearing pins on each side of the boots were replaced with self-aligning roller bearings (fig. 6). Maple filler strips were used to accommodate the smaller member size. A bearing block at each end of the strip assured constant shear in the member inside the boot thereby minimizing the maximum shear stress and reducing the likelihood of a member failing by shear in the boot.

Curvature was measured via a double-arm deflectometer (fig. 7). The two LVDT readings y_1 and y_2 are related to curvature as

$$R = \frac{2(y_2 - y_1)}{a(2\ell + y_1 + y_2)} \qquad (13)$$

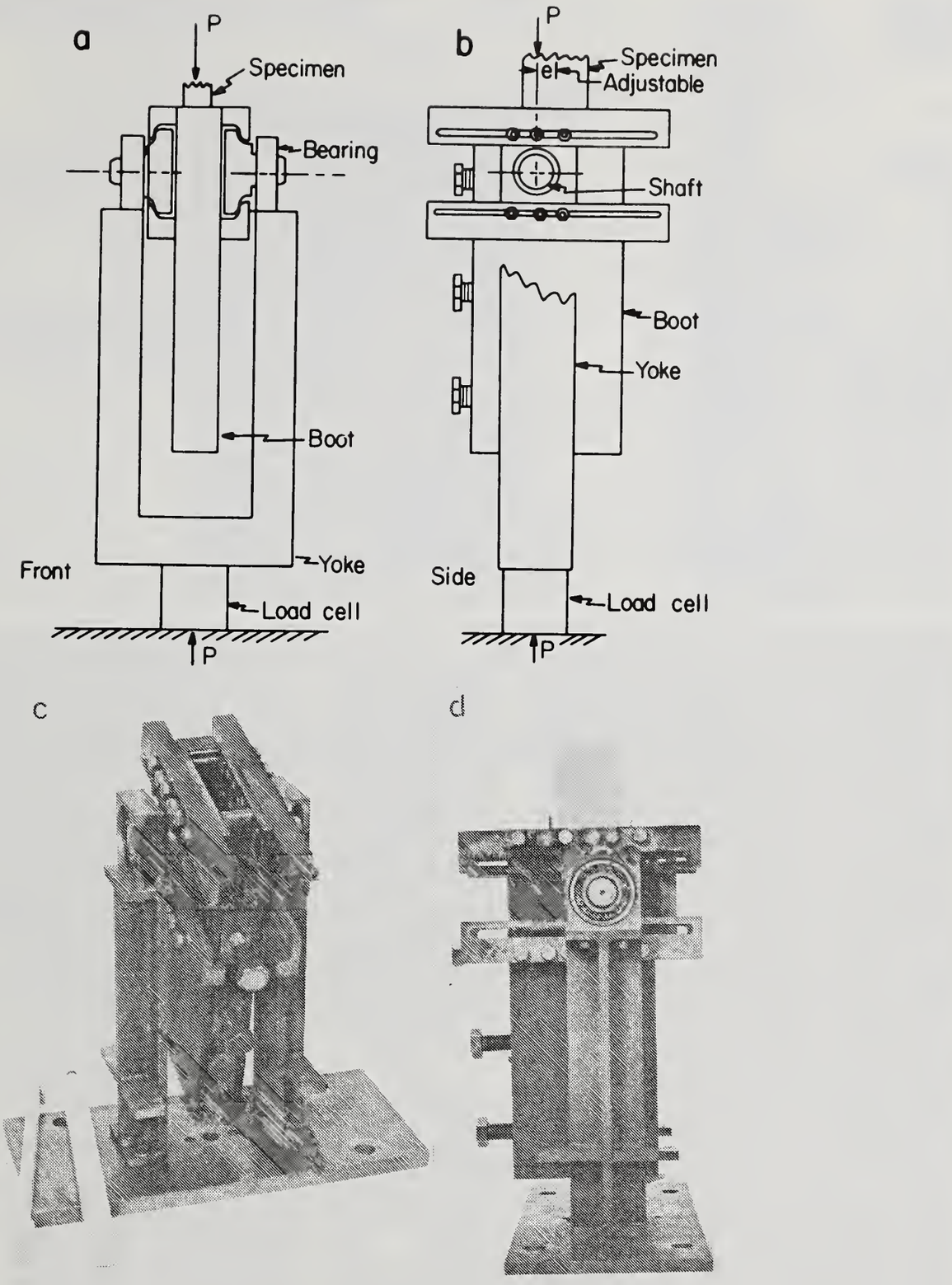

Figure 6.--(a) Front and (b) side view diagrams of boot used as grip for eccentric axial load test. Position of bearings is laterally adjustable. Filler strip adapted boot to smaller size specimen. (c) Side view of bottom boot. (d) Oblique view of boot (maple filler strips have been removed and laid along side) (ML845430, M830384, M830385).

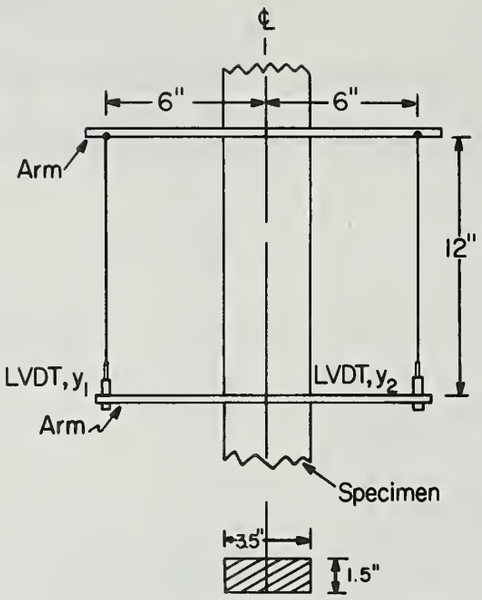

Figure 7.--Deflectometer arrangement used in eccentric axial load test. Rigid arms were clamped to specimen and linear variable differential transformers (LVDT's) were mounted between them 6 inches from center on either side (ML845431).

where R = radius of curvature, ℓ = gage length (12 in.), and a = arm length (12 in.). A third LVDT y_3 measured center deflection relative to the line of action of axial load (fig. 8). Thus the actual moment was

$$M = P(e + y_3) \tag{14}$$

A complete curve of actual moment versus curvature was recorded during each test by an on-line computer and automatically fitted with a Ramberg-Osgood function as given in equations 2 and 3 above. These four parameters were recorded for each specimen as the four-vector $\underline{Y}$ given in equation 5.

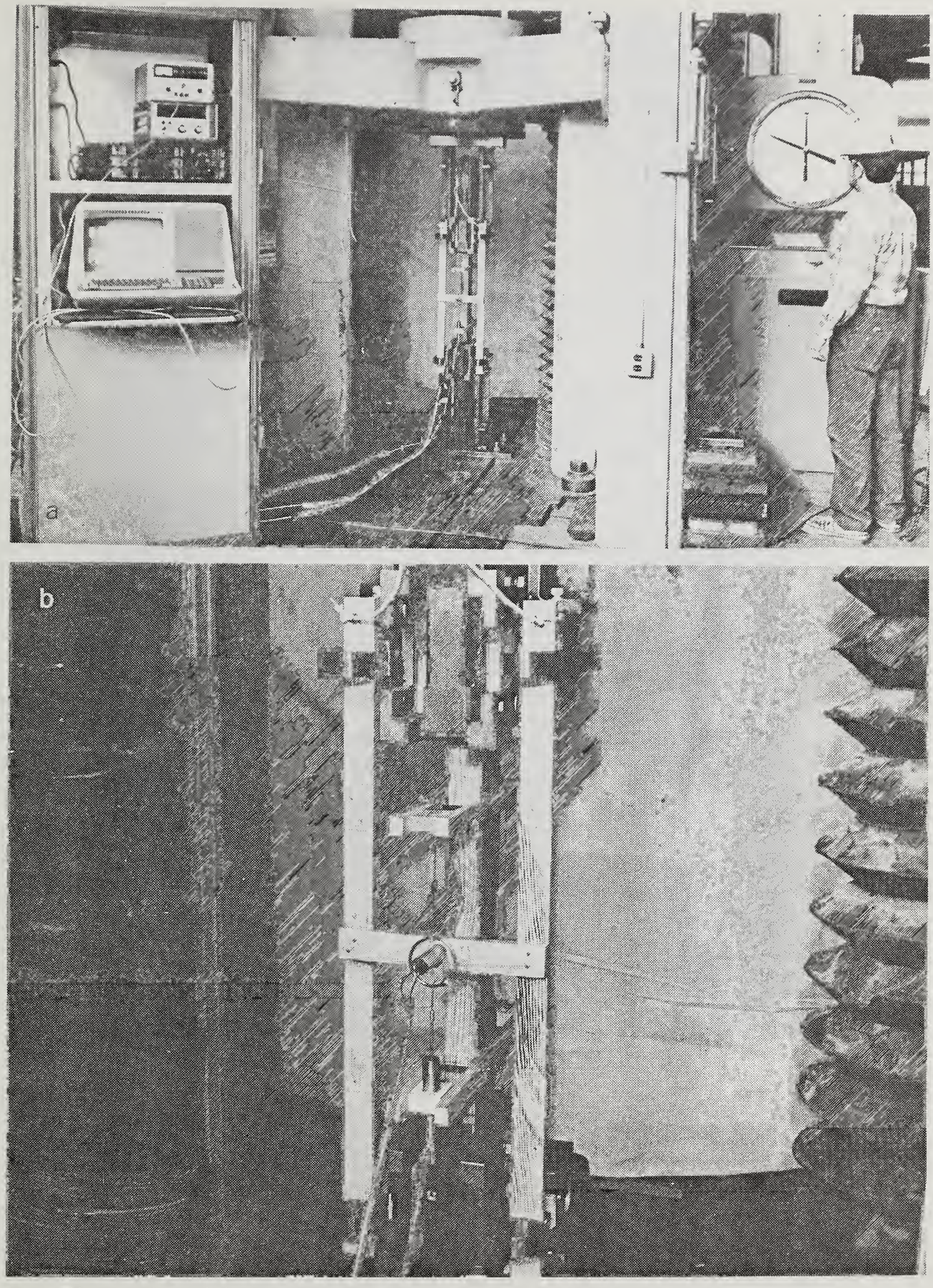

Figure 8.--(a) Fullview and (b) closeup of axial load test set-up.

Verification Tests (longer members)

Seven groups of long specimens, groups 5 through 11, were tested to destruction under eccentric axial load. Several lengths and grades were included (table 1).

Quality rating.--The gage length of each member was marked off into 12-inch elements and each element was rated for quality by measuring VQR and EMOE as described above under Single-Element Tests (short members). When measuring EMOE, the longer overhang was supported by a weight strung over a pulley (fig. 9). The weight was chosen to reduce the shear stress in the element being measured to nearly zero. It was found that the moment-curvature relationship of the element was slightly affected by the presence of an initial constant shear. This non-elastic effect was unexpected and difficult to explain. It may be due to some subtle nonlinearity of the test set-up at low loads. At any rate the pulley system had the effect of producing reasonable and repeatable results.

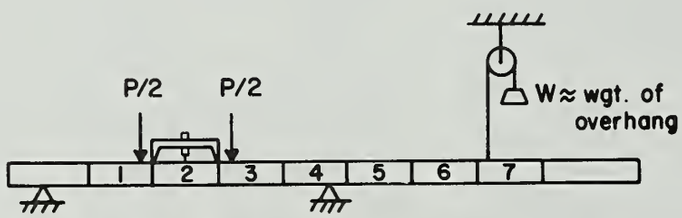

Figure 9.--Sketch of edgewise modulus of elasticity test used to rate quality of each element for members in groups 5 to 11. Overhang was supported by a low-friction pulley. Sketch shows test of second element of seven-element member (ML845432).

Strength tests.--All groups were tested under eccentric axial load at an eccentricity of 0.65 inch (fig. 10). Initial center deflection of each

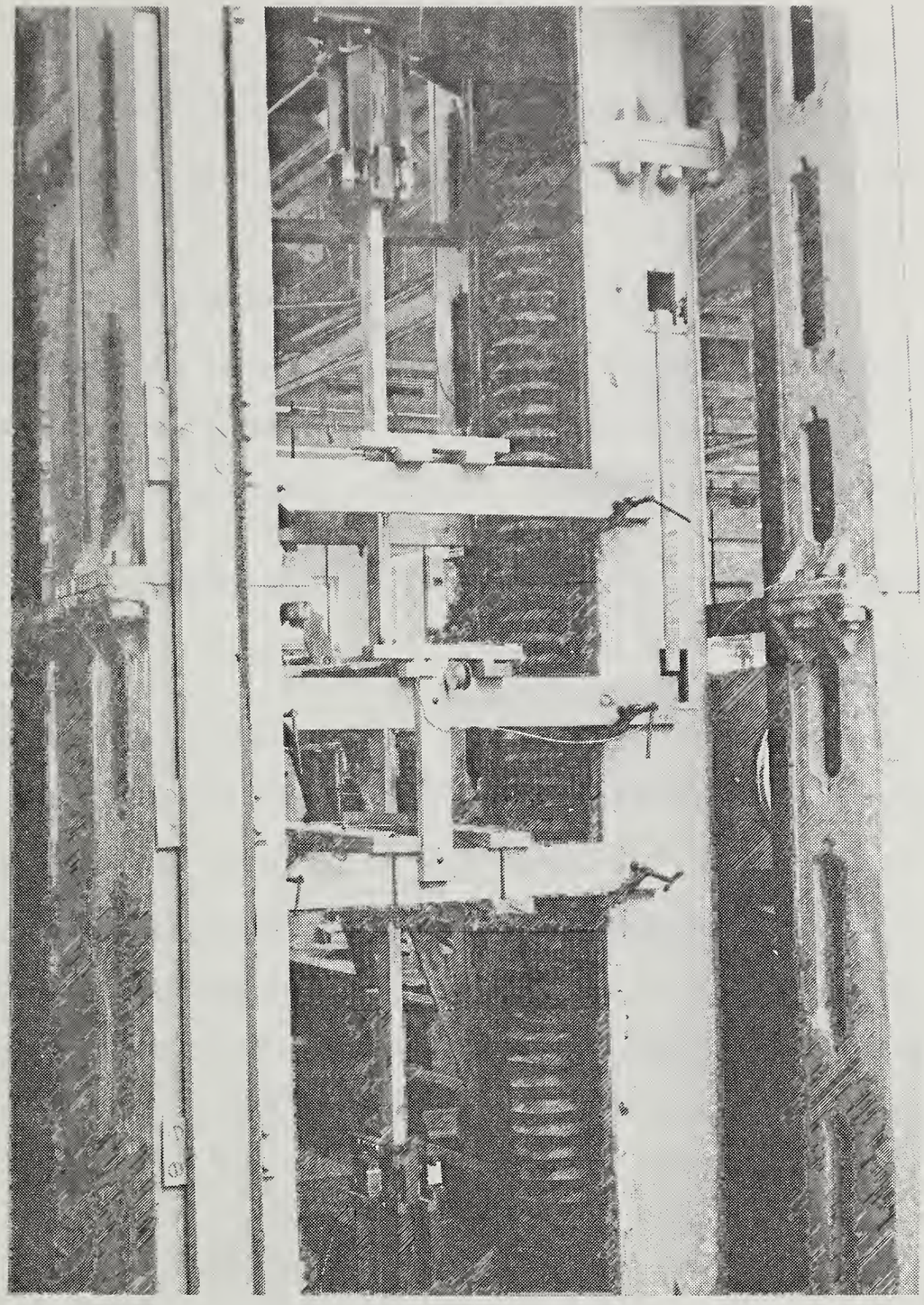

Figure 10.--Photo of test set-up used in destructive eccentric axial load tests for members in groups 5 to 11 (M153014-6).

member was measured and recorded before testing. All members were tested with the initial deflection in the same direction as deflections due to load.

Lateral supports were provided every 30 inches by plexiglass sheets on rollers so that deformation was constrained to be in the strong direction. Only maximum load was recorded.

The top eccentricity of groups 5, 6, and 7 was unintentionally set at zero instead of 0.65 inches. Therefore, the simulator was modified to permit different eccentricities at top and bottom so as not to bias the comparison between simulated and experimental values for these three groups.

EXPERIMENTAL RESULTS

Single-Element Data

The description of these data must be in a form suitable for use as input to the simulation program USBC. These data provide the properties of individual "finite elements," 12 inches long, which are to be assembled into longer members by USBC in each simulation. The quality $\underline{X}$ of each element is given and the properties distribution must provide a corresponding property vector $\underline{Y}$. Following scheme 2 above $\underline{Y}$ was regressed onto $\underline{X}$ and a covariance matrix of $\underline{Y}$ (assumed independent of $\underline{X}$) was calculated. The regression equation is

$$\underline{Y} = \underline{\underline{A}}\,\underline{X} + \underline{B} \tag{15}$$

where $\underline{\underline{A}}$ is a 4 x 2 matrix and $\underline{B}$ is a 4-vector. Denote these statistics as

$$\underline{\underline{A}} \equiv \begin{matrix} S_1 & S_5 \\ S_2 & S_6 \\ S_3 & S_7 \\ S_4 & S_8 \end{matrix}, \quad \underline{B} \equiv \begin{matrix} S_9 \\ S_{10} \\ S_{11} \\ S_{12} \end{matrix} \tag{16}$$

and write the diagonally symmetric covariance matrix as

Table 3.--Southern pine 2 x 4 single-element statistics by regression analysis (see equations 5, 7, and 15)

Statistic	Group			
	1	2	3	4
COEFFICIENT OF (VQR - 7)				
S_1 : $\ell n(EI \times 10^{-6})$	0.03267	0.06707	0.08174	0.01628
S_2 : $\ell n\ M_n$	0.05416	0.08518	0.09794	0.05228
S_3 : $\ell n\ y_u$	0	0	0	0
S_4 : $\ell n\ \ell n\ n$	0	0	0	0
COEFFICIENT OF ($\ell n(EMOE \times 10^{-6}) - 0.45$)				
S_5 : $\ell n(EI \times 10^{-6})$	0.77093	0.70513	0.58970	1.05789
S_6 : $\ell n\ M_u$	0.43827	0.36576	0.39718	0.85722
S_7 : $\ell n\ y_u$	0	0	0	0
S_8 : $\ell n\ \ell n\ n$	0	0	0	0
CONSTANT				
S_9 : $\ell n(EI \times 10^{-6})$	2.2077	2.1182	2.0840	2.0836
S_{10} : ℓn Mu	9.6719	9.8192	10.0010	9.9799
S_{11} : $\ell n\ y_u$	-6.2371	-6.0946	-6.2646	-7.0492
S_{12} : $\ell n\ \ell n\ n$	-0.33278	-0.20361	-0.15208	-0.070745
COVARIANCES (SEE EQUATION 17)				
$S_{13} = var\ (\ell n\ (EI \times 10^{-6}))$	0.27841	0.30392	0.29891	0.45962
$S_{14} = cov\ (\ell n\ (EI \times 10^{-6}),\ \ell n\ M_u)$	0.14753	0.19893	0.23692	0.40795
$S_{15} = cov\ (\ell n\ (EI \times 10^{-6}),\ \ell n\ y_u)$	0	0	0	0
$S_{16} = cov\ (\ell n\ (EI \times 10^{-6}),\ \ell n\ \ell n\ n)$	0	0	0	0
$S_{17} = var\ (\ell n\ M_u)$	0.13762	0.16812	0.22132	0.44823
$S_{18} = cov\ (\ell n\ M_u,\ \ell n\ y_u)$	0	0	0	0
$S_{19} = cov\ (\ell n\ M_u,\ \ell n\ \ell n\ n)$	0	0	0	0
$S_{20} = var\ (\ell n\ y_u)$	0.58099	0.44905	0.56996	0.65012
$S_{21} = cov\ (\ell n\ y_u,\ \ell n\ \ell n\ n)$	-0.12141	-0.035145	-0.012511	0.05062
$S_{22} = var\ (\ell n\ \ell n\ n)$	0.21608	0.15960	0.15123	0.24959

$$\underline{\underline{\Omega}} \equiv \begin{bmatrix} S_{13} & S_{14} & S_{15} & S_{16} \\ & S_{17} & S_{18} & S_{19} \\ (\text{SYM}) & & S_{20} & S_{21} \\ & & & S_{22} \end{bmatrix} \tag{17}$$

Table 3 shows these statistics S_i for each of groups 1 to 4.

Note that Y_3 ($\ell n\ y_u$) and Y_4 ($\ell n\ \ell n\ n$) did not correlate significantly with $\underline{X}$ and hence their regression equations were reduced to simple constants (mean values). Likewise the covariances between Y_3 or Y_4 and Y_1 or Y_2 were insignificantly small and were arbitrarily set to zero (lines 15, 16, 18, and 19 of table 3). Thus the quality vector $\underline{X}$ can only predict stiffness and strength; ductility and knee shape were independent of the chosen quality measures.

The dependence of properties upon eccentricity, e, was previously modeled (Zahn 1982) as a simple parabola fitted by least squares to data at four values of e. However, a parabola can easily give large errors if extrapolated too far beyond the range in which it was fitted. In this study, the statistics S_i for each of groups 1 to 4 (table 3) were fitted by the following function (table 4).

$$S_i = A_i + \left(B_i + \frac{C_i}{e} \right) \exp\left(- \frac{D_i}{e} \right), \quad i = 1,22 \tag{18}$$

A sketch of this function for S_6 shows its behavior (fig. 11). Note from equations 5, 7, and 15 that S_6 is the coefficient relating ℓnM_u to $\ell n[\text{EMOE} \times 10^{-6}] - 0.45$.

Constants A_i through D_i were fitted as follows:

Table 4.--Coefficients of fitted equation 18--
dependence of properties on
eccentricity

i	A_i	B_i	C_i	D_i
1	0.03367	-0.017389	0.32232	2.2438
2	0.05416	-0.0018801	0.25436	2.0967
3	0	0	0	0
4	0	0	0	0
5	0.77093	0.28696	-2.6475	3.5800
6	0.43827	0.41895	-1.2101	2.3897
7	0	0	0	0
8	0	0	0	0
9	1.6251	-0.13155	-1.5580	1.7498
10	9.0956	0.13260	-0.18801	0.39740
11	-6.2371	-0.81210	1.6885	1.8165
12	-0.33278	0.26204	-0.025667	0.60426
13	0.27841	0.18121	-0.11187	1.0
14	0.14753	0.26042	-0.12070	1.0
15	0	0	0	0
16	0	0	0	0
17	0.13762	0.31061	-0.12293	1.8170
18	0	0	0	0
19	0	0	0	0
20	0.58100	0.069001	-0.42766	1.0
21	-0.12141	0.12141	0.097373	0.93066
22	0.21608	0.033510	-0.41737	1.9164

1. $A_i = S_i$ at e = 0, but because no data were obtained at e = 0, data at e = 0.65 were substituted. The lack of data at e = 0 makes it difficult to simulate pure compression accurately, about which more will be said under Simulated Interaction of Bending and Compression below.

2. $A_i + B_i = S_i$ at $e = \infty$. Group 4 data provide S_i at $e = \infty$.

3. C_i and D_i were then chosen by trial to fit groups 2 and 3 (e = 1 and e = 2.25).

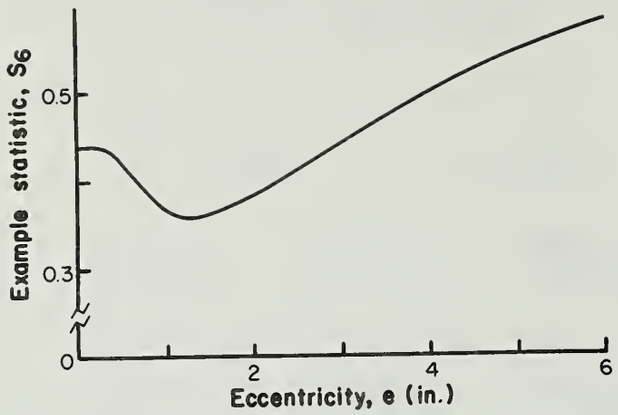

Figure 11.--Graph of equation 18 showing how S_6 depends on eccentricity (ML845433).

Constants A_i through D_i could have been chosen by trial so that equation 18 exactly fit the four data points but then the value at e = 0 would sometimes be very different from the values obtained in groups 1 to 4. The above scheme was adopted to ensure numerical stability at e = 0. The penalty for doing this is that realistic results cannot be obtained at e = 0.

Because the S_i do not depend linearly on the constants A_i through D_i, I decided to subtract central values from VQR and $\ell n(EMOE \times 10^{-6})$ as shown in equation 7 so that the constant $\underline{B}$ in equation 15 could ensure accurate representation of $\underline{X}$ in the central part of its range. $\underline{B}$ is, of course, S_9 through S_{12} (see equation 16).

The single-element data are not representative of southern pine 2 x 4's but rather were obtained from a sample chosen to cover an extreme range of quality. Hence these statistics are not very useful for any other purpose than as input to USBC.

Verification Data

These data were obtained for two main reasons: 1) to verify the accuracy of USBC and 2) to provide representative samples of quality vector $\underline{X}$ for use

in simulating the interaction of bending and compression strength at several lengths and grades. These results will be discussed in separate sections. Here I present the quality data (table 5) and show a typical example of how X varied along the length of one member (fig. 12).

Table 5.--Summary of quality data, long members

$$\text{Table entry}^1 = \begin{matrix} VQR_{max}, \ EMOE \times 10^{-6}_{max} \\ \underline{VQR_{avg}}, \ \underline{EMOE \times 10^{-6}_{avg}} \\ VQR_{min}, \ EMOE \times 10^{-6}_{min} \end{matrix}$$

Gage length	Grade			Average[2]
	1	2	3	
Ft				
5		9.30, 2.02 8.53, 1.76 7.43, 1.49	8.97, 1.82 7.75, 1.49 5.49, 1.04	9.15, 1.93 8.17, 1.63 6.52, 1.28
7	9.76, 2.46 8.76, 2.08 7.45, 1.73		9.61, 2.07 8.67, 1.64 7.33, 1.20	9.69, 2.27 8.72, 1.87 7.39, 1.47
9		9.38, 1.98 8.32, 1.58 6.46, 1.14		9.38, 1.98 8.32, 1.58 6.46, 1.14
11	9.64, 2.48 8.76, 2.03 7.23, 1.54	9.69, 1.99 8.08, 1.62 5.72, 1.20		9.67, 2.24 8.42, 1.83 6.48, 1.37
Average[2]	9.69, 2.47 8.76, 2.05 7.31, 1.61	9.50, 1.99 8.26, 1.63 6.33, 1.24	9.25, 1.97 8.29, 1.58 6.58, 1.13	9.53, 2.15 8.43, 1.76 6.71, 1.34

[1]Max and min are per specimen. Table entry is average for a group.

[2]Averages are weighted by number of elements per table entry.

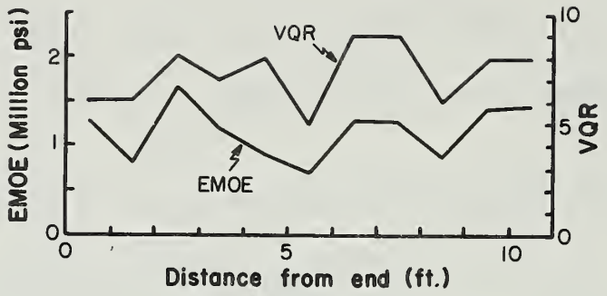

Figure 12.--Variation of quality along length of a typical, grade 2 southern pine 2 x 4 (ML845434).

Although they were not obtained for this purpose, the failure load data of groups 5 to 11 exhibit the effects of length and grade at one particular load ratio (figs 13 and 14). Strength decreases with lower grade or with greater length, as one would expect. These results are not definitive because the sample size is small. The longer members could be compared with elastic theory but no such comparison is presented here because prebuckling displacements have a dominant effect on the failing load and the secant formula does not accurately model these displacements for nonhomogeneous members.

DEVELOPMENT OF IMPROVED SIMULATOR USBC

One of the objectives of this study was to develop an improved finite-element simulator capable of reproducing both the mean and the variance of verification data. The finite element simulator used previously (Zahn 1982), was modified in the following ways (appendix II):

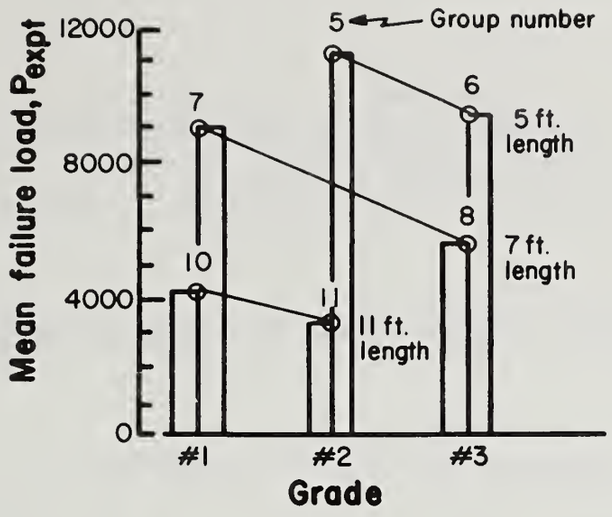

Figure 13.--Summary of experimental results for groups 5 to 11. Average failing load of each group is plotted against grade of lumber. Each point is the average of all members within a single group not counting members that failed in the grips. All of these data were obtained at an eccentricity of 0.65 inch except that groups 5, 6, and 7 were tested with top eccentricity = 0 and bottom eccentricity = 0.65 inch (ML845435).

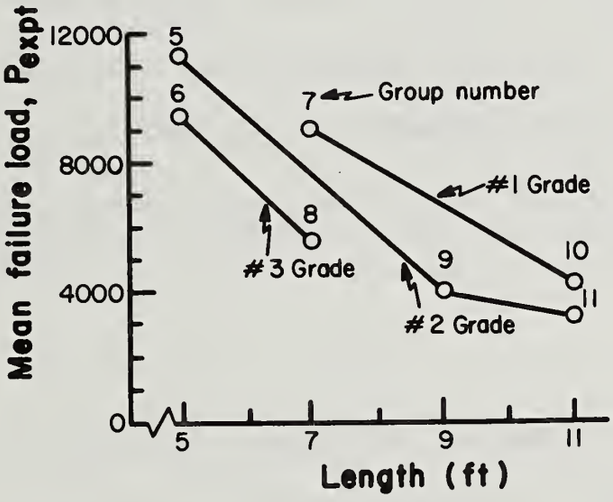

Figure 14.--Summary of experimental results for groups 5 to 11. Average failing load of each group is plotted against length of member. Each point is the average of all members within a single group, not counting members that failed in the grips. All of these data were obtained at an eccentricity of 0.65 inch except that groups 5, 6, and 7 were tested with top eccentricity = 0 and bottom eccentricity = 0.65 inch (ML845436).

Minor Modifications

1. The number of elements was made an input variable.

2. Two quality indices, VQR and EMOE, were input for each element instead of just E_r.

3. Top and bottom eccentricities were made input variables, not necessarily equal.

4. The initial shape of the member was assumed to be a sine wave rather than perfectly straight. Initial center deflection Δ_o was made an input variable.

Introducing visual quality rating VQR as a second measure of quality did not contribute much. This can be seen by comparing the regression of $\underline{Y}' \equiv [\ell n(EI \times 10^{-6}), \ell n\ M_u]$ onto $\underline{X} = [VQR, \ell n(EMOE \times 10^{-6})]$ with the regression of $\underline{Y}'$ onto $\ell n(EMOE \times 10^{-6})$ alone (table 6). Note that the residual sum of squares is not improved much by the addition of VQR.

In addition to these minor modifications, the representation of the element property distribution and its dependence on quality $\underline{X}$ and eccentricity e were improved in various ways until overall model performance was deemed to be acceptable. These major changes are discussed next.

Major Modifications

The functional dependence of $\underline{Y}$ upon eccentricity has already been presented in equation 18. The other major modification was the change from scheme 1 (joint $\underline{Y}$, $\underline{X}$ distribution) to scheme 2 (regression analysis) and ultimately to scheme 3 (deterministic).

Table 6.--Comparison of regressions with and without VQR[1]

Group	Statistic	Regression Coefficient of VQR	Regression Cofficient of ℓn (EMOE x 10^{-6})	Regression constant	Residual sum of squares, percent
1	ℓn (EI x 10^{-6})	--	0.868	1.83	68.4
		0.0339	0.769	1.63	68.8
	ℓn M_u	--	0.606	9.41	65.6
		0.0541	0.447	9.09	68.9
2	ℓn (EI x 10^{-6})	--	0.881	1.74	80.6
		0.0671	0.705	1.33	83.1
	ℓn M_u	--	0.589	9.58	64.9
		0.0852	0.366	9.06	72.4
3	ℓn (EI x 10^{-6})	--	0.770	1.76	80.9
		0.0817	0.590	1.25	85.2
	ℓn M_u	--	0.613	9.75	69.1
		0.0979	0.397	9.14	77.6
4	ℓn (EI x 10^{-6})	--	1.10	1.59	95.7
		0.0163	1.06	1.49	95.8
	ℓn M_u	--	0.980	9.55	78.3
		0.0523	0.857	9.23	79.3

[1]First line shows regression excluding VQR and second line shows regression including VQR.

In the previous study of western hemlock, I used a full Monte-Carlo simulation of 8-foot-long members and found after testing the members to failure that the simulator was able to reproduce the mean of the experimental values but underestimated their variability (fig. 15). These results were obtained by the simulator SIMTST of the previous study. The first version of USBC, call it USBC1, resembled SIMTST except that it used the regression equation 15

to get the mean of $\underline{Y}$ and then randomly selected from a 4-variate normal distribution (table 3).

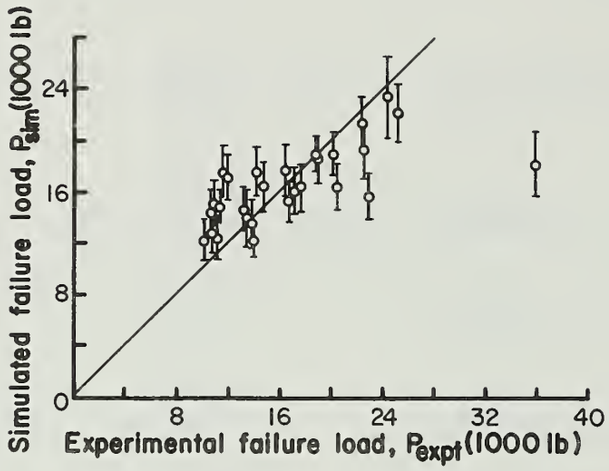

Figure 15.--Scatter diagram of output of simulator SIMTST versus corresponding experimental values of western hemlock 2 x 6's. Simulated failing load of each member is an average of 30 Monte Carlo simulations. Reproduced from Zahn (1982) (ML845437).

When I applied this scheme to group 5 (5-ft No. 2 grade southern pine 2 x 4's), I found that it still underestimated variability (fig. 16) just as SIMTST did. To account for this, consider the sources of variation in output P_{sim} of a simulator program:

1. Variation in input (quality vector $\underline{X}$ of each element), and

2. Additional variation in mechanical properties (vector $\underline{Y}$ of each element) not explained by $\underline{X}$.

The second source of variation is present in any single simulation of a Monte Carlo program such as SIMTST or USBC1. However, when each member is simulated many times and the results are averaged, this variation is averaged out!

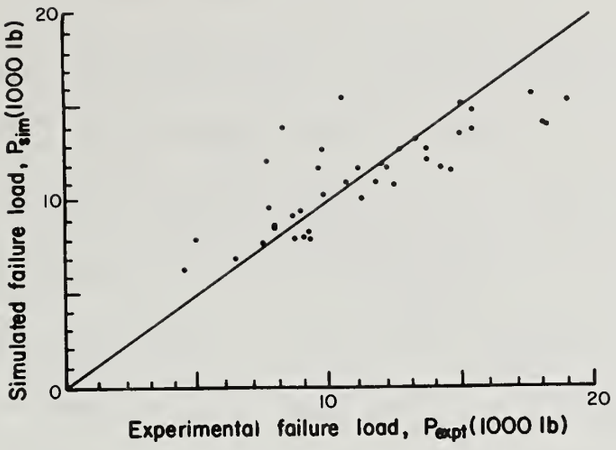

Figure 16.--Output from first version of simulator USBC versus corresponding experimental values of southern pine 2 x 4's in group 5. Simulated failing load of each member is an average of 40 Monte Carlo simulations (ML845438).

The obvious solution is to perform a single Monte-Carlo simulation of each member. However, wood properties vary so greatly that no conclusions could be drawn from the results of a single random simulation. Therefore the second version, USBC2, simulated each member only once and used the most likely value for $\underline{Y}$ found from the regression equation 8 of $\underline{Y}$ onto $\underline{X}$. The covariance matrix was not used. The results resemble those obtained by USBC1 (fig 17).

Thus, the result is essentially the same whether one uses maximum likelihood inputs (USBC2) or obtains maximum liklihood outputs (USBC1). Either way variability will always be underestimated. This is because the random variation about the most likely value (source 2 above) is being lost. This information is present in the covariance matrix of $\underline{Y}$ but in USBC1 it was averaged out and in USBC2 it was never used.

How then can one avoid losing this source of variation? It can be done by simulating each member only once with $\underline{Y}$ obtained from $\underline{X}$ by an orthogonal least squares analysis in place of the linear regression equation 8. That is

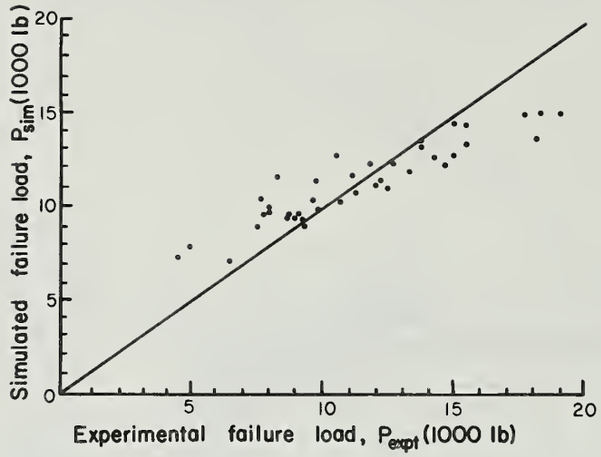

Figure 17.--Output from second version of simulator USBC versus corresponding experimental values of southern pine 2 x 4's in group 5. Here each member was simulated only once using maximum likelihood estimates for each element's material properties (ML845439).

$$\underline{Y} = \underline{\underline{A}}' \underline{X} + \underline{B}' \tag{19}$$

where $\underline{\underline{A}}'$ and $\underline{B}'$ are fitted by the orthogonal least squares method (appendix III). This method uses both the mean vector and the covariance matrix of $\underline{Y}$ to construct the matrix $\underline{\underline{A}}'$ and the vector $\underline{B}'$. The resulting equation 19 treats $\underline{X}$ and $\underline{Y}$ equally (either can be used to predict the other) and is simply the closest-fitting linear relationship between $\underline{X}$ and $\underline{Y}$. When used to predict $\underline{Y}$ from a given $\underline{X}$ it has the desirable property of preserving the full variation in $\underline{Y}$ corresponding to a given variation in $\underline{X}$. In this application that property is more advantageous than the property of maximum likelihood, which treats the variables unsymmetrically and always understates the variability of the predicted variable.

However, care must be taken when using orthogonal least squares. The "perpendicular distance" of a point from a plane in space is meaningful only if the coordinates of that space are commensurate--that is, if the variables

plotted along the two coordinate axes are physically the same and expressed in the same units. Obviously that is not the case here where $\underline{Y}$ consists of a flexural rigidity and a moment and $\underline{X}$ consists of a quality rating and an edgewise modulus of elasticity. However, we have taken natural logarithms of all dimensional quantities thereby making the choice of unit an additive constant. Now only the base of the logarithm affects the scale of the variables and one need only be consistent in this choice for all variables.

Equation 19 was fitted to the data for southern pine 2 x 4's in each of groups 1 to 4 (table 7) where

$$\underline{\underline{A}}' \equiv \begin{bmatrix} S_1' & S_5' \\ S_2' & S_6' \\ S_3' & S_7' \\ S_4' & S_8' \end{bmatrix}, \quad \underline{B}' = \begin{bmatrix} S_9' \\ S_{10}' \\ S_{11}' \\ S_{12}' \end{bmatrix} \tag{20}$$

These statistics were fitted by the function

$$S_i' = A_i' + \left[B_i' + \frac{C_i'}{e} \right] \exp\left(- \frac{D_i'}{e} \right), \quad i = 1,12 \tag{21}$$

(table 8).

The final version of USBC used orthogonal least squares in place of regression and simulated each member only once (fig. 18). Note that both mean and variance of the simulated failure loads now agree well with those of experimental values.

Table 7.--Southern pine 2 x 4 single-element statistics by orthogonal least squares (see equations 19 and 20)

Statistic	Group			
	1	2	3	4
	COEFFICIENT OF (VQR - 7)			
S'_1 : ℓn (EI x 10^{-6})	-0.060649	0.019442	0.051453	0.0024324
S'_2 : ℓn M_u	0.020103	0.048149	0.068109	0.0083417
S'_3 : ℓn y_u	0	0	0	0
S'_4 : ℓn ℓn n	0	0	0	0
	COEFFICIENT OF (ℓn (EMOE x 10^{-6}) - 0.45)			
S'_5 : ℓn (EI x 10^{-6})	1.2539	0.93307	0.72568	1.1211
S'_6 : ℓn M_u	0.61515	0.54417	0.53183	1.0582
S'_7 : ℓn y_u	0	0	0	0
S'_8 : ℓn ℓn n	0	0	0	0
	CONSTANT			
S'_9 : ℓn (EI x 10^{-6})	2.2297	2.1322	2.0915	2.0909
S'_{10} : ℓn M_u	9.6799	9.8300	10.008	10.003
S'_{11} : ℓn y_u	-6.2371	-6.0946	-6.2646	-7.0492
S'_{12} : ℓn ℓn n	-0.33278	-0.20361	-0.15208	-0.070745

Table 8.--Coefficients of fitted equation 21--dependence of properties on eccentricity

i	A'_i	B'_i	C'_i	D'_i
1	-0.060649	0.063081	0.41725	1.7913
2	0.020103	-0.011761	0.35543	2.5058
3	0	0	0	0
4	0	0	0	0
5	1.2539	-0.13280	-2.9502	2.2628
6	0.61515	0.44305	-1.6597	2.8414
7	0	0	0	0
8	0	0	0	0
9	2.2297	-0.13880	-0.28545	1.4705
10	9.6799	0.32310	1.5275	2.5120
11	-6.2371	-6.0946	-6.2646	-7.0492
12	-0.33278	-0.20361	-0.15208	-0.070745

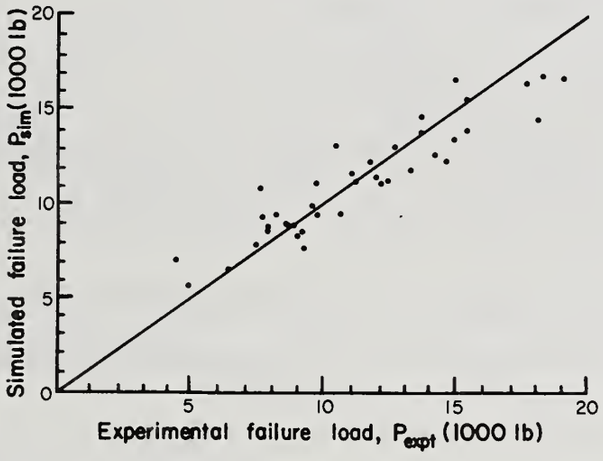

Figure 18.--Output from final version of simulator USBC versus corresponding experimental values of southern pine 2 x 4's in group 5. Here each member was simulated once using orthogonal least squares estimates for each element's material properties (ML845440).

VERIFICATION OF SIMULATOR USBC

USBC allows the material properties of each element to change with increasing load by making the transformed material property vector $\underline{Y}$ a function of element eccentricity. To be conservative, the moment capacity at a given curvature is only allowed to decrease, not increase, as load is increased. That is, the properties can only deteriorate, not improve, as a result of increased load. This may be unduly conservative for long members, because they experience mostly bending stresses and the material properties under pure bending are usually better than under combined bending and compression. As a result, the model should err on the conservative side with the error increasing with length.

The southern pine 2 x 4 data from groups 1 to 4 were represented by an orthogonal least squares equation dependent upon eccentricity. The quality measures for each element of a specimen in groups 5 to 11 were input and a destructive load test was numerically simulated yielding an output failing load P_{sim} for each specimen (figs. 18-19). Because these samples are not large enough to establish behavior in the low tails of the distributions, it is best to look only at the behavior of the means and variances. Therefore I also compared simulated and experimental values of the mean plus or minus one standard deviation for each group (fig. 20).

Note that USBC reproduces both the mean and the variance of each group quite well. As expected, it becomes progressively more conservative (underestimates the mean) as length is increased. Because elastic behavior at great length is fairly well modeled by elastic theory, some conservatism in this region is not a drawback. USBC also appears to underestimate the strength

of grade No. 1. On the whole though, the modeling of length and grade is extremely good, especially in regions where such modeling is most valuable--namely lower grades and shorter lengths.

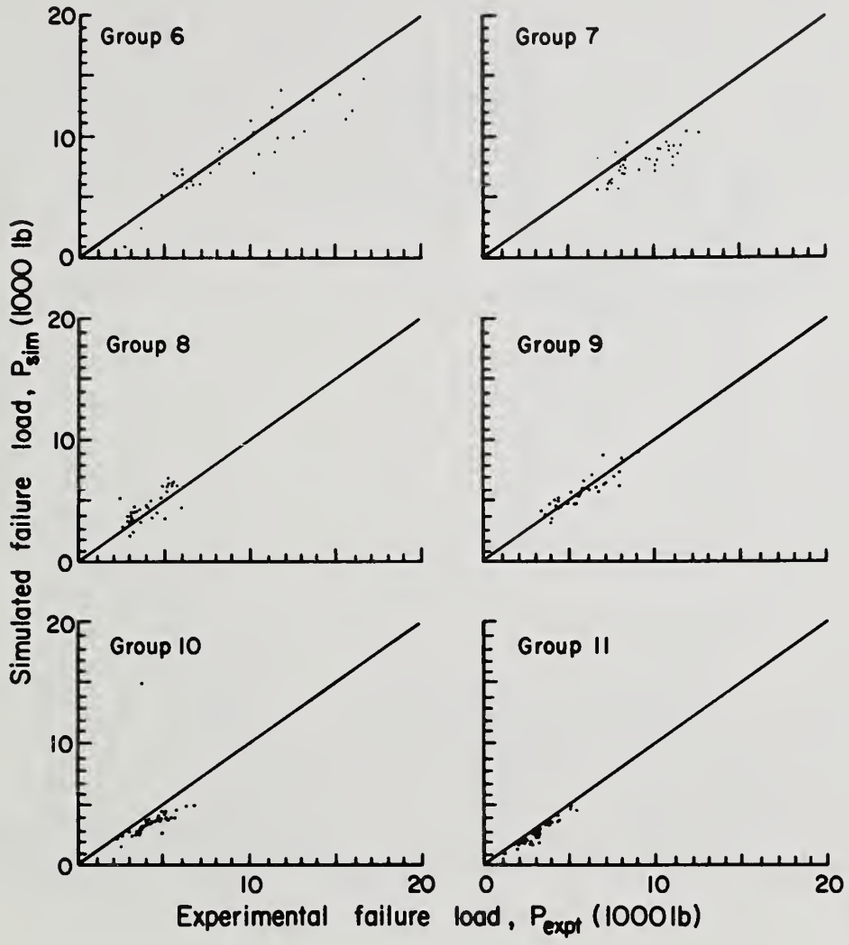

Figure 19.--USBC output values versus corresponding experimental values for groups 6 to 11 (ML845445).

SIMULATED INTERACTION OF BENDING AND COMPRESSION

To simulate the interaction of bending and compression at a given length and grade one needs a sample of input quality measures for that length and grade. The quality measures (VQR and EMOE) of groups 5 to 11 can be used for

this purpose. Although 40 is a small sample size for a material as variable as lumber, it is sufficient to establish the mean.

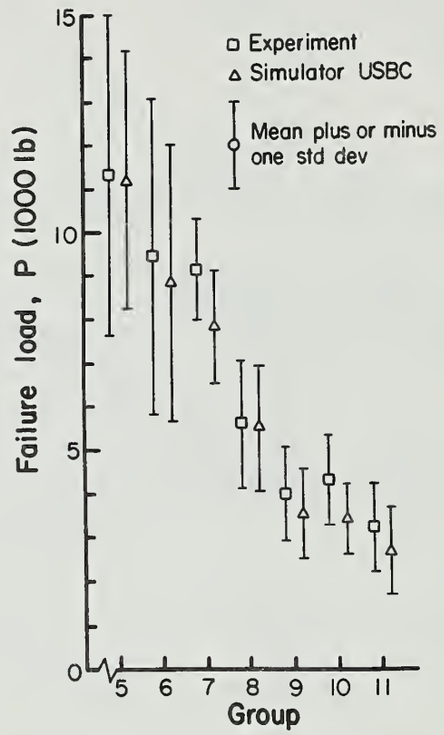

Figure 20.--Summary comparison of USBC output and experimental loads. The mean value plus or minus one standard deviation is shown for groups 5 to 11 (ML845441).

Comparison with Linear Interaction Equation

The ratio of nominal bending moment to axial compression can be changed by varying the eccentricity (equation 1). Simulator USBC was run at various eccentricities for groups 5 to 11 and the results show that the linear interaction equation used in design is conservative at every length and grade (fig. 21). It appears to be less conservative at longer lengths and higher grades, but here the simulator itself is known to be conservative.

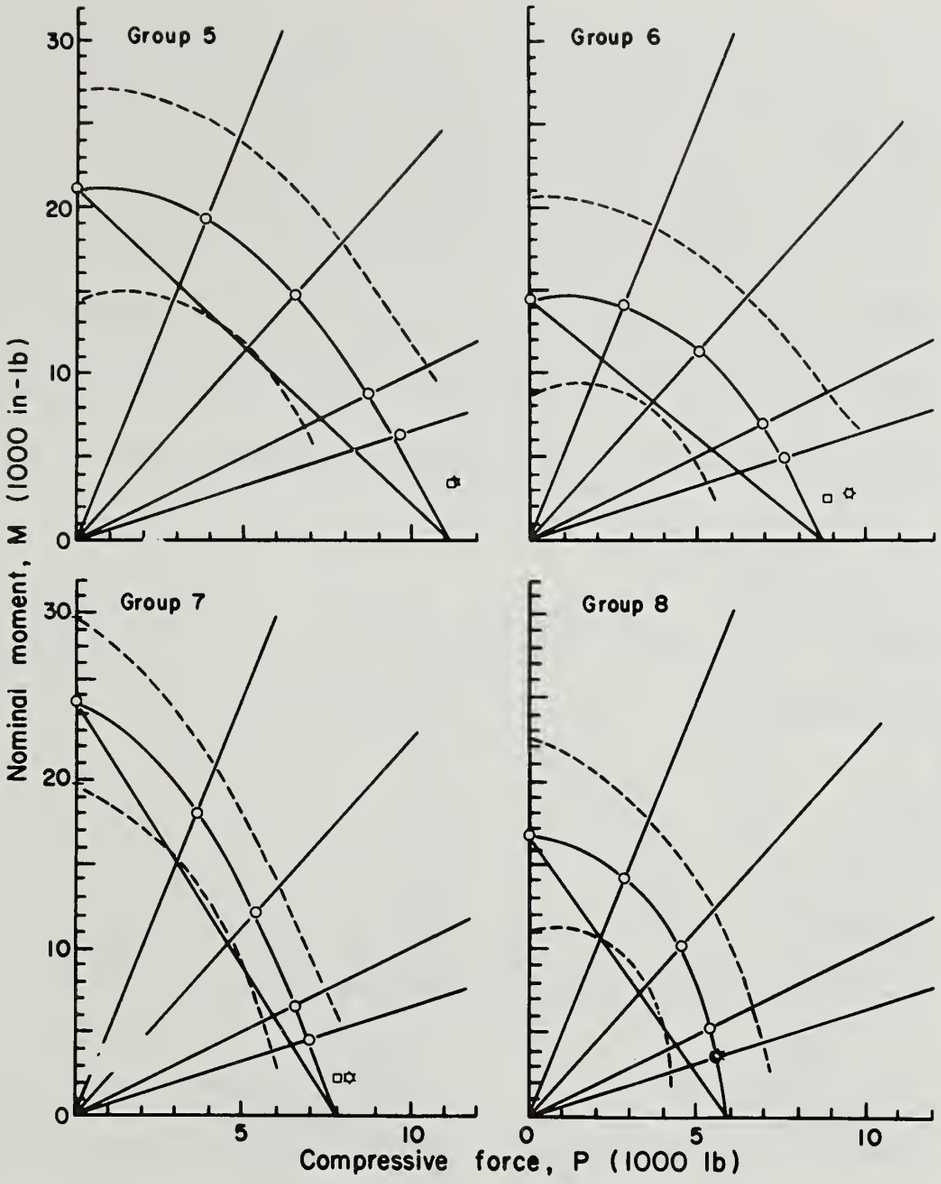

Figure 21a.--Simulated interaction of bending and compression for groups 5 through 8. Straight line is design equation. The mean plus or minus one standard deviation is shown for each eccentricity (ratio of moment to axial load) (ML845447).

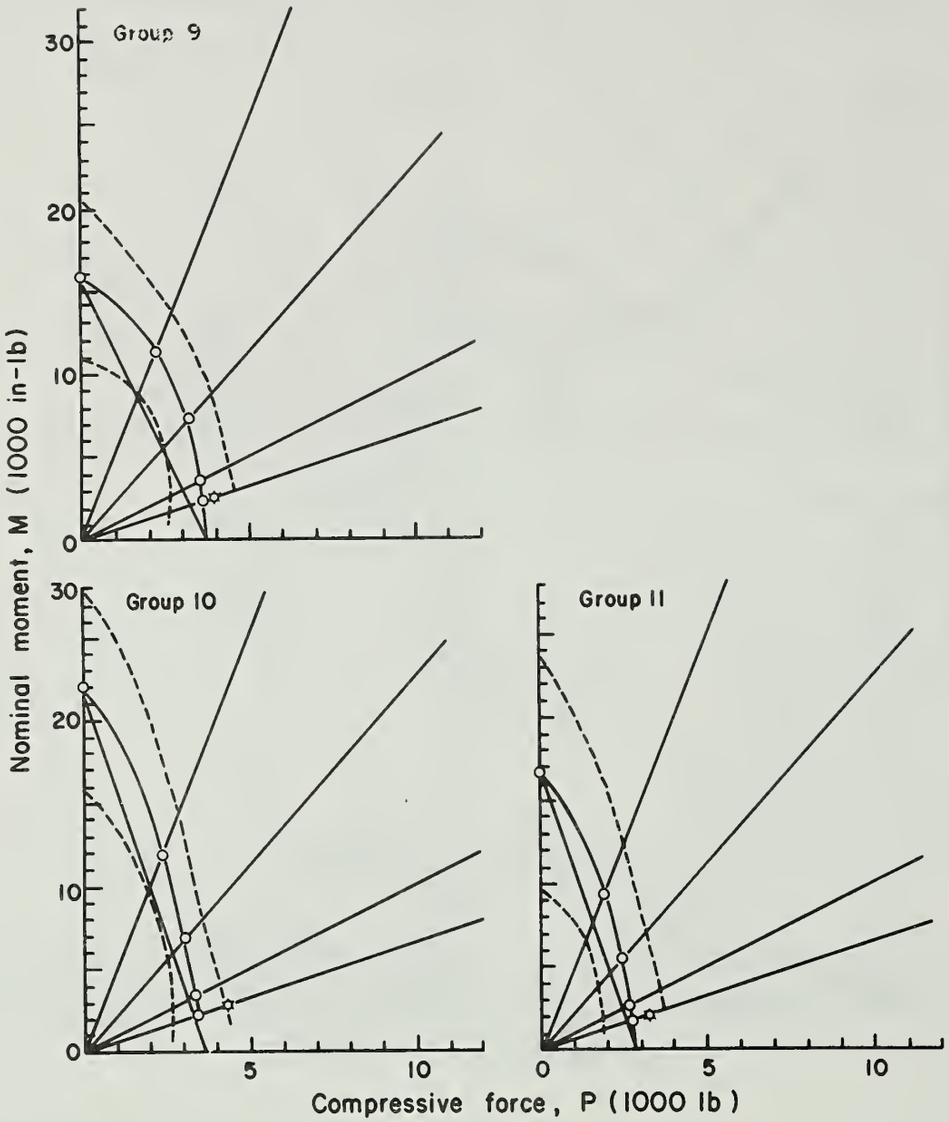

Figure 21b.--Simulated interaction of bending and compression for groups 9 through 11. Straight line is design equation. The mean plus or minus one standard deviation is shown for each eccentricity (ratio of moment to axial load) (ML845446).

Effect of Length and Grade Upon Interaction

The effects of length and grade upon the interaction curve are of interest. Therefore I replotted figure 21 with normalized coordinates

obtained by dividing moment by moment capacity in pure bending and axial load by axial load capacity (figs. 22 and 23). Because axial load capacity cannot be simulated by USBC (no data were taken at zero eccentricity) that value was estimated by extrapolation on figure 21. No data were taken in pure compression for two reasons: first, the main interest lay in applications where bending predominates and second, the simulator USBC models only bending behavior with bending properties dependent on superposed compression.

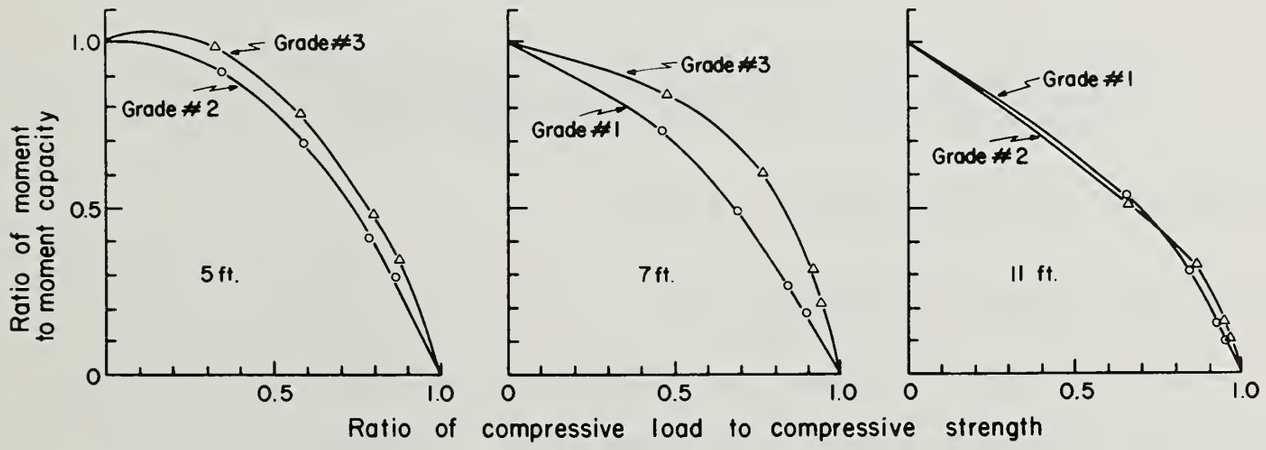

Figure 22. Normalized interaction curves of southern pine 2 x 4's showing effect of grade (ML845449).

Note that normalization via bending and compressive strengths did not completely remove the effects of length and grade as one might have hoped. The curves are humped at the pure bending end for shorter members of lower grade and are humped at the pure compression end of the curves for longer members of higher grade. Thus, if a nonlinear interaction equation were to be used in design, the shape of the curve would have to be dependent upon length and grade. Otherwise only a slight nonlinearity, conservative for all lengths and grades, would have to be adopted.

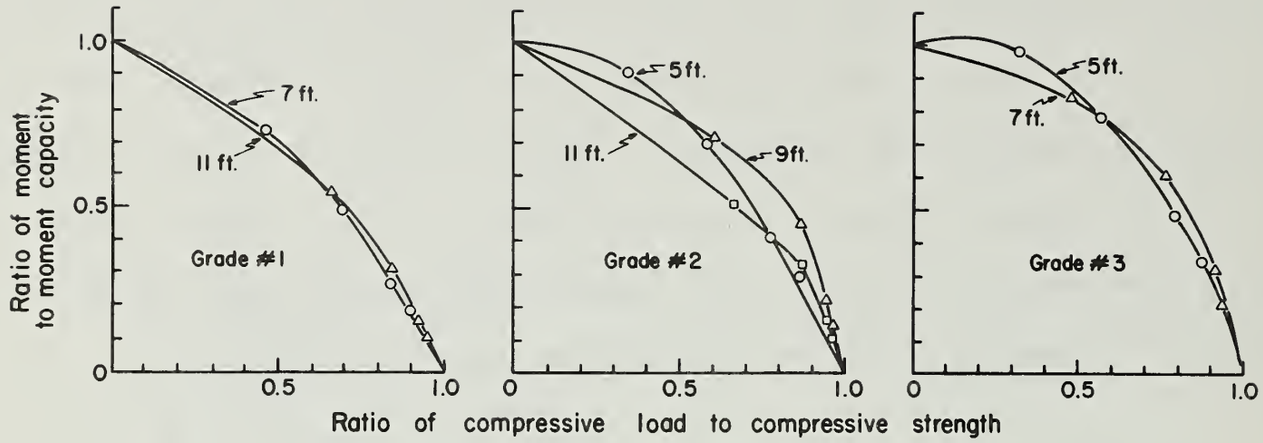

Figure 23.--Normalized interaction curves of southern pine 2 x 4's showing effect of length (ML845448).

REANALYSIS OF WESTERN HEMLOCK 2 x 6 DATA

Interaction of Bending and Compression

The interaction of bending and compression for 8-foot western hemlock 2 x 6's was simulated by Zahn (1982) (fig. 24). In that study the input was a smaller sample (28) of mixed grades with only a single quality measure, E_r, for each element. Because USBC is superior to the simulator SIMTST used in that study, I decided to reanalyse the western hemlock data using orthogonal least squares (tables 9 and 10). USBC was able to closely reproduce both mean and variance of experimental data (fig. 25).

The interaction curve obtained by USBC (fig. 26) looks more reasonable than one obtained by SIMTST (fig. 24) when one compares them with the western hemlock single-element data. The single-element data S_6' of group 4 in table 9 shows that SIMTST severely underestimated bending strength. That error resulted from a poor representation of the dependence of element properties upon eccentricity. A simple parabola in 1/e is not as well behaved as the function given in equation 21.

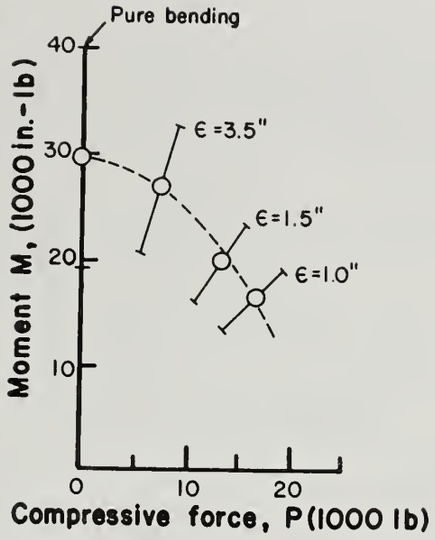

Figure 24.--Interaction of bending and compression in western hemlock 2 x 6's as simulated by SIMTST. Reproduced from Zahn (1982) (ML845442).

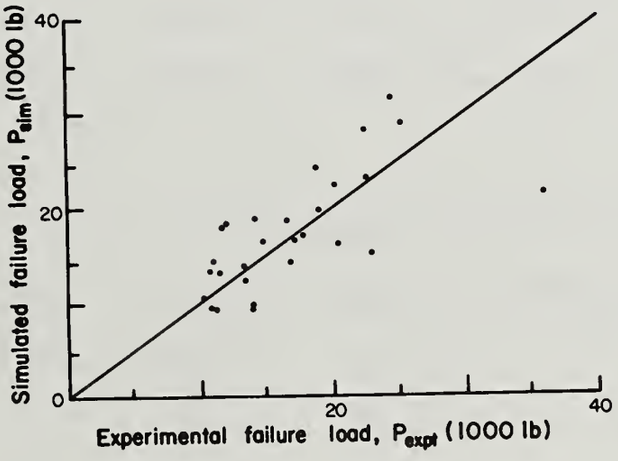

Figure 25.--Output of simulator USBC versus corresponding experimental values for western hemlock 2 x 6's of mixed grades. Compare figure 15 (ML845443).

Table 9.--Western hemlock 2 x 6 data pool statistics by orthogonal least squares (see equations 19 and 20)

Statistic	Group			
	1	2	3	4
	COEFFICIENT OF VQR			
S'_1 : $\ell n\ (EI \times 10^{-6})$	0	0	0	0
S'_2 : $\ell n\ M_u$	0	0	0	0
S'_3 : $\ell n\ y_u$	0	0	0	0
S'_4 : $\ell n\ \ell n\ n$	0	0	0	0
	COEFFICIENT OF $(\ell n\ (E_r \times 10^{-6}) - 0.031)$			
S'_5 : $\ell n\ (EI \times 10^{-6})$	2.0071	1.8686	1.5283	1.6835
S'_6 : $\ell n\ M_u$	1.4950	1.5456	1.9392	3.5388
S'_7 : $\ell n\ y_u$	0	0	0	0
S'_8 : $\ell n\ \ell n\ n$	0	0	0	0
	CONSTANT			
S'_9 : $\ell n\ (EI \times 10^{-6})$	3.7492	3.6585	3.6371	3.7676
S'_{10} : $\ell n\ M_u$	10.482	10.586	10.767	10.662
S'_{11} : $\ell n\ y_u$	-6.839	-6.715	-6.772	-7.887
S'_{12} : $\ell n\ \ell n\ n$	0.702	0.758	0.701	0.433

Table 10.--Coefficients of fitted equation 21--
dependence of western hemlock
2 x 6 properties on eccentricity

i[1]	A'_i	B'_i	C'_i	D'_i
1	0	0	0	0
2	0	0	0	0
3	0	0	0	0
4	0	0	0	0
5	2.0071	-0.32360	-4.4836	3.5470
6	1.4950	2.0438	-1.3019	2.6853
7	0	0	0	0
8	0	0	0	0
9	3.7492	0.018400	-0.63083	1.9099
10	10.482	0.18000	2.1475	3.1081
11	-6.8390	-1.0480	2.8537	2.6784
12	0.70200	-0.26900	0.60029	1.7776

[1]The values for i = 1 to 4 are zero because VQR was not measured.

Because only a single sample of mixed grades and one length is available for western hemlock 2 x 6's, nothing can be concluded about the effects of length and grade for that material.

Species Effect

It would be fortunate if data for one species could be used to simulate another species, given that quality measures had been obtained for a particular length and grade of that other species. Two things characterize the material properties distribution of a particular species: 1) the dependence of material properties on quality measures (orthogonal least squares equation relating $\underline{Y}$ to $\underline{X}$) and 2) the dependence of material properties on eccentricity (how bending

properties are affected by simultaneous compression). This second characteristic is expressed by the magnitudes of the constants A_i' to D_i'.

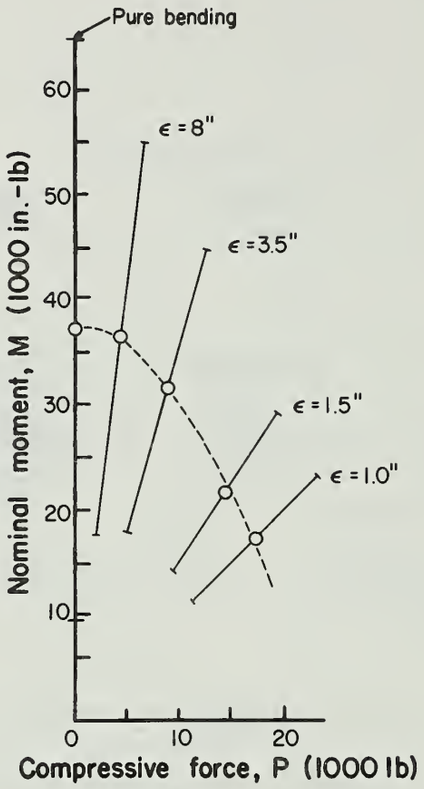

Figure 26.--Interaction of bending and compression in western hemlock 2 x 6's as simulated by USBC. Compare figure 24 (ML845444).

Unfortunately, the single-element data for western hemlock and southern pine cannot be directly compared. The difference in cross-section size could easily be adjusted but the difference in quality measures EMOE and E_r is profound. There is no possible way to infer one from the other. Nevertheless it can be shown that the two species <u>are</u> significantly different. Because group 4 of each species was tested in pure bending, it follows that EI and EMOE should be related as

$$\frac{EI}{I} = EMOE \qquad (22)$$

Thus we can compare the slope of the orthogonal least squares line relating $\ell n\ M_u$ to $\ell n(EI/I)$ for group 4 of each species. If the species are interchangeable, these slopes must be the same. If they are not the same, species must have a significant effect. For southern pine this slope was calculated to be 0.986; for western hemlock it is 2.169. Because this slope is independent of cross-section size, we conclude that the bending strength of western hemlock is much more sensitive to EMOE than is southern pine. That is a very significant species difference. Applying the southern pine single-element data to the simulation of western hemlock would grossly underestimate variability in strength.

SUMMARY

Simulator USBC

Given the element property distribution for a given size and species of lumber, and a sample of input nondestructive quality measures for a given grade and length, the simulator USBC presented here can accurately simulate the effects of length and grade upon the strength of lumber under combined bending and compression. This simulator is an improved version of SIMTST developed by Zahn (1982). The most significant change was the introduction of orthogonal least squares analysis and determinate simulation in place of regression analysis (or the use of a conditional distribution) and Monte Carlo simulation. This change not only improved the accuracy but also reduced the cost of running the program by an order of magnitude.

Input Data for USBC

Future studies of this interaction of bending and compression can use the element property data presented in this report. Data for 12-inch southern pine 2 x 4 elements are presented in tables 7 and 8. Reanalyzed data for 18-inch western hemlock 2 x 6 elements is presented in tables 9 and 10. Representative samples of quality measured nondestructively for seven groups of southern pine and one of western hemlock are on magnetic tape at Forest Products Laboratory. The southern pine data are summarized in table 5. These data can be used to study the interaction of bending and compression strength for the lengths and grades shown in table 1. If additional samples of element quality are obtained nondestructively for western hemlock 2 x 6's or southern pine 2 x 4's, the element property data presented here can be used with program USBC to predict the interaction of bending and compression for those new samples.

Interaction of Bending and Compression

A plot of bending moment versus axial compressive force at failure under combined loading exhibits the interaction of bending and compression strength. The representative samples of quality data gathered here were used as input to USBC to exhibit this interaction for several lengths and grades of southern pine 2 x 4's. The results showed that the interaction curve possesses an upward hump whose shape and location depend on the length and grade of material (figs. 22 and 23).

Design Implications

Although the exact shape of the interaction equation depends on length and grade, it may be possible to fit a conservative equation to the simulated

interaction data (fig. 21). These data show that the linear interaction equation

$$\frac{M}{M_u} + \frac{P}{P_u} = 1 \qquad (21)$$

used as the basis of the current design code is conservative for all lengths and grades. Before recommending a less conservative equation for design, however, three things require further investigation: 1) the interaction of buckling modes in long members that are not laterally restrained as were the members in this study, 2) the effect of different types of loading that could produce bending, and 3) the strength of in-grade lumber under pure compression and lateral restraint.

REFERENCES

1. Gerhards, C. C., "Effect of high-temperature drying on bending strength of yellow-poplar 2 x 4's," Forest Products Journal, Vol. 33, No. 2, Feb., 1983, pp. 61-67.

2. Morrison, D. F., Multivariate Statistical Methods, McGraw-Hill Book Co., New York; 1967, pp. 80-85.

3. Pearson, K., "On lines and planes of closest fit to systems of points in space," Philosophical Magazine, Series 6, Vol. 2, 1901, pp. 559-572.

4. Ramberg, W., and Osgood, W. E., "Description of stress-strain curves by three parameters," NACA TN-902. Washington DC: National Advisory Committee for Aeronautics; July 1943. 13 pp. plus figs.

5. Zahn, J. J., "Strength of lumber under combined bending and compression," Res. Pap. FPL 391, Forest Prod. Lab., Forest Serv., USDA, Madison, Wis.; 1982.

APPENDIX I--NOTATION

$\underline{\underline{A}}$, $\underline{B}$	Regression coefficients. See equation 8.
$\underline{\underline{A}}'$, $\underline{B}'$	Orthogonal least squares coefficients. See equation 9.
A_i, B_i, C_i, D_i	Coefficients that describe dependence on eccentricity. See equation 18.
A_i', B_i', C_i', D_i'	Coefficients that describe dependence on eccentricity. See equation 21.
a	Deflectometer span. See equation 11 or equation 13.
c	One half of largest dimension of cross section.
$\underline{E}$	Quality vector. See equation 6.
EI	Initial slope of moment-curvature relationship. See equation 2.
EMOE	Edgewise modulus of elasticity, psi.
e	Eccentricity of axial load.
$\underline{F}$	Material property vector. See equation 4.
I	Principal moment of inertia.
ℓ	Gage length, 12 inches.
M	Bending moment.
M_u	Ultimate bending moment.
m	Number of statistics needed to specify $\underline{Y}(\underline{X})$.
n	Knee shape parameter. See equation 2.
P	Axial compressive force.
P_u	Ultimate axial compressive force.
P_{expt}	Experimental value of P_u.
$\bar{P}_{expt}$	Average of P_{expt}.
P_{sim}	Simulated value of P_u.
R	Radius of curvature.

S_i	Property distribution statistic. See equations 16 and 17.
S_i'	Property distribution statistic. See equation 20.
VQR	Visual quality rating (Gerhards 1983).
$\underline{X}$	Transformed quality vector. See equation 7.
X	$\frac{Mc}{I}$.
$\underline{Y}$	Transformed material property vector. See equation 5.
y	$\frac{c}{R} - \frac{Mc}{I}$.
Y_u	Value of y at ultimate (maximum) load.
y_1, y_2, y_3	LVDT readings.
Δ_o	Initial center deflection of long members.
$\underline{\underline{\Omega}}$	Covariance matrix of $\underline{Y}$.

APPENDIX II--SPECIAL FINITE-ELEMENT ANALYSIS USED IN USBC

Figure A1 shows a free body diagram of axially loaded member. Let initial deflection be

$$v = e_o + \left(\frac{e_L - e_o}{L} \right) \chi + \Delta_o \sin \frac{\pi \chi}{L} \qquad \text{(A1)}$$

where e_o = eccentricity at $\chi = 0$; e_L = eccentricity at $\chi = L$; Δ_o = initial center deflection measured relative to ends of member; L = length; and χ = axial coordinate. Let y = deflection due to load. Then total deflection measured from line of action of axial load P is y + v.

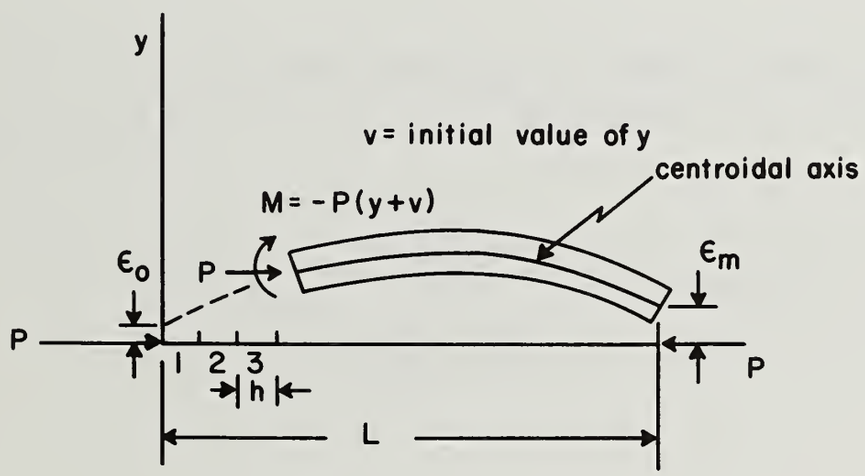

Figure A1.--Free-body diagram of member under eccentric axial load.

Divide member into m finite elements of length h. The bending of the n-th element due to load is

$$(EI)_n \, y_n'' = - P(y_n + v), \quad (n - 1)\, h \leq \chi \leq nh \qquad \text{(A2)}$$

where $y_n(\chi)$ is $y(\chi)$ in the n-th element and primes denote differentiation with respect to χ. Let p_n denote nodal values of y. Then the boundary values of y_n are

$$y_n = p_{n-1} \text{ at } \chi = (n-1)\, h \tag{A3}$$

$$y_n = p_n \text{ at } \chi = nh \tag{A4}$$

The solution of equations A1 to A4 is

$$y_n = \frac{q_n \cos \lambda_n (n-1)h - q_{n-1} \cos \lambda_n nh}{\sin \lambda_n h} \sin \lambda_n \chi$$

$$+ \frac{-q_n \sin \lambda_n (n-1)h + q_{n-1} \sin \lambda \; nh}{\sin \lambda_n h} \cos \lambda_n \chi$$

$$- e_o - \left(\frac{e_L - e_o}{L} \right) \chi - \left(\frac{\lambda_n^2}{\lambda_n^2 - \frac{\pi^2}{L^2}} \right) \Delta_o \sin \frac{\pi \chi}{L} \tag{A5}$$

where

$$q_j \equiv P_j + e_o + \left(\frac{e_L - e_o}{L} \right) jh + \frac{\lambda_n^2}{\lambda_n^2 - \frac{\pi^2}{L^2}} \Delta_o \sin \frac{\pi jh}{L} \tag{A6}$$

and

$$\lambda_n \equiv \frac{P}{(EI)_n} \tag{A7}$$

Match slopes at n-th node:

$$y'_n = y'_{n+1} \text{ at } \chi = nh \tag{A8}$$

Inserting equation A5 into equation A8 yields the following system of equations:

$$\left(\frac{-\lambda_n}{\sin \lambda_n h} \right) q_{n-1} + \left(\frac{\lambda_n \cos \lambda_n h}{\sin \lambda_n h} + \frac{\lambda_{n+1} \cos \lambda_{n+1} h}{\sin \lambda_{n+1} h} \right) q_n + \left(\frac{-\lambda_{n+1}}{\sin \lambda_{n+1} h} \right) q_{n+1}$$

$$= \frac{\left(\lambda_{n+1}^2 - \lambda_n^2 \right) \frac{\pi^2}{L^2}}{\left(\lambda_n^2 - \frac{\pi^2}{L^2} \right)\left(\lambda_{n+1}^2 - \frac{\pi^2}{L^2} \right)} \Delta_o \frac{\pi}{L} \cos \frac{\pi n h}{L}, \quad n = 1, m \tag{A9}$$

System A8 has two more unknowns than equations. However, the overall boundary conditions are

$$p_o = 0 \tag{A10}$$

$$p_m = 0 \tag{A11}$$

so that

$$q_o = e_o \tag{A12}$$

$$q_m = e_L \tag{A13}$$

and then system A9, A12, A13 has m + 1 equations in the m + 1 unknowns q_o through q_m.

Except for the refinement of initial deflections and the new representation of the single-element property distribution, the computing method of USBC is exactly like that of SIMTST described in Zahn (1982).

APPENDIX III--ORTHOGONAL LEAST SQUARES

The problem of fitting a linear equation to data so as to minimize the sum of squares of deviates measured perpendicular to the fitted hyper-plane was first solved by K. Pearson (1901). Only the results are presented here. For further details see Morrison (1967).

To find matrix $\underline{\underline{A}}'$ and vector $\underline{B}'$ such that

$$\underline{Y} = \underline{\underline{A}}' \, \underline{X} + \underline{B}' \tag{B1}$$

where $\underline{Y}$ is an n-vector and $\underline{X}$ is an m-vector, proceed as follows:

1. Let

$$\underline{Z} = \begin{bmatrix} \underline{Y} \\ \underline{X} \end{bmatrix} \tag{B2}$$

be an (m + n)-vector for which we possess a sample of size N, namely $\underline{Z}_i$, i = 1 to N. Compute the mean vector $\overline{\underline{Z}}$ and the sample covariance matrix $\underline{\underline{S}}$. Partition the mean vector as

$$\overline{\underline{Z}} = \begin{bmatrix} \overline{\underline{Y}} \\ \overline{\underline{X}} \end{bmatrix} \tag{B3}$$

2. Find the unit eigenvectors and eigenvalues of $\underline{\underline{S}}$ and order them from smallest to largest:

$$\underline{\underline{S}} \, \underline{V}_i = \lambda_i \underline{V}_i, \; \left| \underline{V}_i \right| = 1, \; i = 1, \; n + m \tag{B4}$$

$$\lambda_1 \leq \lambda_2 \leq \cdots \leq \lambda_{n+m} \tag{B5}$$

3. Form the orthogonal matrix $\underline{\underline{T}}$ using the $\underline{V}_i$ as column vectors

$$\underline{\underline{T}} = \begin{bmatrix} \uparrow & \uparrow & & \uparrow \\ \underline{V}_1 & \underline{V}_2 & \cdots & \underline{V}_{n+m} \\ \downarrow & \downarrow & & \downarrow \end{bmatrix} \tag{B6}$$

and partition it as follows:

$$\underline{\underline{T}} = \begin{bmatrix} \underline{\underline{T}}_{yy} & \underline{\underline{T}}_{yx} \\ \underline{\underline{T}}_{xy} & \underline{\underline{T}}_{xx} \end{bmatrix} \tag{B7}$$

where $\underline{\underline{T}}_{yy}$ is n x n, $\underline{\underline{T}}_{yx}$ is n x m, and $\underline{\underline{T}}_{xy}$ is m x n and $\underline{\underline{T}}_{xx}$ is m x m.

4. Calculate $\underline{\underline{A}}'$ and $\underline{B}'$ from the formulas

$$\underline{\underline{A}}' = \underline{\underline{T}}_{yx}\, \underline{\underline{T}}_{xx}^{-1} \tag{B8}$$

$$\underline{B}' = \overline{\underline{Y}} - \underline{\underline{A}}\, \overline{\underline{X}} \tag{B9}$$